

Structure-based optimization of coumarin hA3 adenosine receptor antagonists

Maria João Matos, Santiago Vilar, Saleta Vazquez-Rodriguez, Sonja Kachler, Karl-Norbert Klotz, Michela Buccioni, Giovanna Delogu, Lourdes Santana, Eugenio Uriarte, and Fernanda Borges

J. Med. Chem., **Just Accepted Manuscript** • DOI: 10.1021/acs.jmedchem.9b01572 • Publication Date (Web): 18 Nov 2019

Downloaded from pubs.acs.org on November 18, 2019

Just Accepted

"Just Accepted" manuscripts have been peer-reviewed and accepted for publication. They are posted online prior to technical editing, formatting for publication and author proofing. The American Chemical Society provides "Just Accepted" as a service to the research community to expedite the dissemination of scientific material as soon as possible after acceptance. "Just Accepted" manuscripts appear in full in PDF format accompanied by an HTML abstract. "Just Accepted" manuscripts have been fully peer reviewed, but should not be considered the official version of record. They are citable by the Digital Object Identifier (DOI®). "Just Accepted" is an optional service offered to authors. Therefore, the "Just Accepted" Web site may not include all articles that will be published in the journal. After a manuscript is technically edited and formatted, it will be removed from the "Just Accepted" Web site and published as an ASAP article. Note that technical editing may introduce minor changes to the manuscript text and/or graphics which could affect content, and all legal disclaimers and ethical guidelines that apply to the journal pertain. ACS cannot be held responsible for errors or consequences arising from the use of information contained in these "Just Accepted" manuscripts.

Structure-based Optimization of Coumarin hA₃ Adenosine Receptor Antagonists

Maria João Matos,^{a,b,*} Santiago Vilar,^b Saleta Vazquez-Rodriguez,^b Sonja Kachler,^c Karl-Norbert Klotz,^c Michela Buccioni,^d Giovanna Delogu,^e Lourdes Santana,^b Eugenio Uriarte,^{b,f} Fernanda Borges^{a,*}

^a CIQUP/Department of Chemistry and Biochemistry, Faculty of Sciences, University of Porto, 4169-007 Porto, Portugal

^b Department of Organic Chemistry, Faculty of Pharmacy, University of Santiago de Compostela, 15782 Santiago de Compostela, Spain

^c Institute of Pharmacology and Toxicology, University of Würzburg, 97078 Würzburg, Germany

^d School of Pharmacy, Medicinal Chemistry Unit, University of Camerino, 62032 Camerino, Italy

^e Department of Life Sciences and Environment - Section of Pharmaceutical Sciences, University of Cagliari, 09124 Cagliari, Italy

^f Instituto de Ciencias Químicas Aplicadas, Universidad Autónoma de Chile, 7500912 Santiago, Chile

Abstract. Adenosine receptors participate in many physiological functions. Molecules that may selectively interact with one of the receptors are favorable multifunctional chemical entities to treat or decelerate the evolution of different diseases. 3-Arylcoumarins have already been studied as neuroprotective agents by our group. Here, differently 8-substituted 3-arylcoumarins are complementarily studied as ligands of adenosine receptors, performing radioligand binding assays. Among the synthesized

compounds, selective A_3 receptor antagonists were found. 3-(4-Bromophenyl)-8-hydroxycoumarin (compound **4**) displayed the highest potency and selectivity as A_3 receptor antagonist ($K_i = 258$ nM). An analysis of its X-ray diffraction provided detailed information on its structure. Further evaluation of a selected series of compounds indicated that it is the nature and position of the substituents that determine their activity and selectivity. Theoretical modeling calculations corroborate and explain the experimental data, suggesting this novel scaffold can be involved in the generation of candidates as multitarget drugs.

Keywords: 3-Arylcoumarins • Perkin reaction • Perkin-Oglialoro reaction • Adenosine antagonists • Molecular modeling

INTRODUCTION

Adenosine acts as a common control of several cellular functions.¹ This purine regulates fundamental pathophysiological activities through four receptor subtypes (A_1 , A_{2A} , A_{2B} and A_3).² Adenosine is the endogenous, nonselective agonist which remains shortly in the human body, while inosine –its metabolite– being metabolised by adenosine deaminase, weakly interacts with the A_3 receptor.³

Adenosine receptors are GPCR (G protein-coupled receptors) that are being described as potential therapeutic targets for a wide range of pathologies.⁴ From cancer to brain diseases, these receptors are involved in immunological and inflammatory conditions.^{5,6} There is a huge variety of chemicals designed as adenosine receptor ligands, both directly acting as agonists, antagonists, and indirect modulators.⁷ Regadenoson (CVT-3146) was proposed as selective A_{2A} agonist. This molecule has been playing an interesting role inducing stress for imaging techniques in cardiology.⁸ Istradefylline (KW-6002) was approved in Japan for Parkinson's disease. This xanthine derivate proved to be a strong A_{2A} antagonist.⁹

The increasing knowledge on the structure and mechanisms of A₃ receptor has given fundamental pieces of evidence to validate it as a promising therapeutic target.¹⁰ This enables a rational design on robust A₃ selective antagonists as therapeutic solutions for several diseases.¹¹ Recent reports manifest an important role for A₃ receptor in mediating adenosine function at the central nervous system.^{12,13} A₃ receptors are also described as inducers of strong anti-inflammatory activity in animal models.¹⁴ These particular effects aroused our attention, since our group has been active in the research of age-related pathologies, in particular vascular, inflammatory and neurodegenerative diseases.¹⁵ Based on the background of our research group regarding differently substituted coumarins as potential adenosine receptor ligands,^{16,17,18,19,20,21} and in the potential of some of these compounds as neuroprotectors and enzymatic inhibitors related to neurodegenerative disorders (i.e. acetylcholinesterase, butyrylcholinesterase and monoamine oxidase B), in this work we report a group of coumarins bearing a wide variety of substituents as modulators of adenosine receptors. In particular, the revealing achievements of our last work on the interesting activity of 8-substituted 3-arylcoumarins (Figure 1) have been the inspiration for the progression of this study.²¹ Design, synthesis, pharmacological evaluation, docking calculations, and structure-activity relationship exploration of a family of 8-substituted 3-arylcoumarins, were performed.

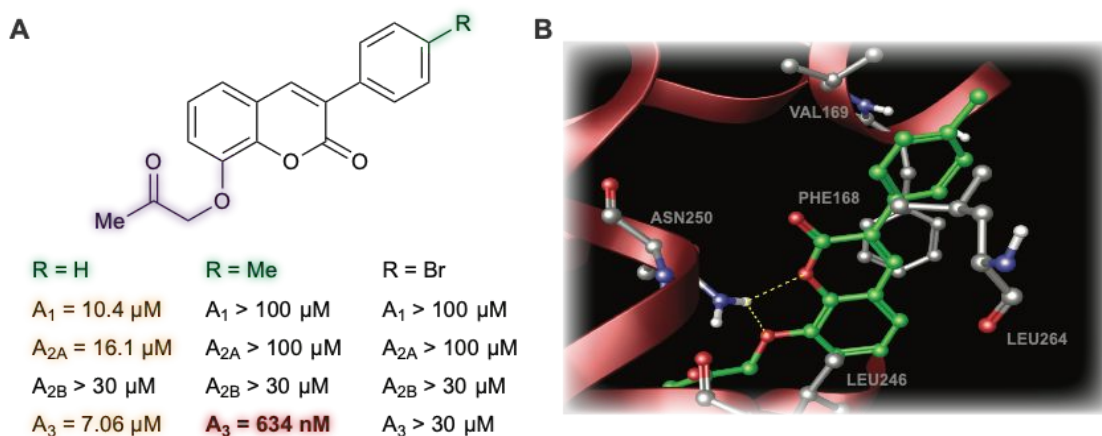


Figure 1. Previous results from the group on the potential of 8-substituted 3-arylcoumarins as adenosine ligands at adenosine 7TM receptors. **A.** Three 8-(2-oxopropoxy)-3-arylcoumarins with different affinity profiles. **B.** Hypothetical binding mode for 8-(2-oxopropoxy)-3-(*p*-tolyl)coumarin in the hA₃ protein pocket (template for the hA₃ homology model: 3EML). Color code: pale orange – micromolar range; red – nanomolar range.

RESULTS AND DISCUSSION

Chemistry. Molecules **1-27** were prepared based on the synthetic strategies described in Figure 2A. In general, these compounds were obtained by a classic Perkin (compounds **1-3**, **5-14**, **16** and **17**) and Perkin-Oglialoro (compounds **18-22**) reactions. Further hydrolysis of the ethoxy (compounds **4** and **15**) and acetoxy derivatives (compounds **23-27**) allowed the obtention of the hydroxyl derivatives.^{22,23,24,25}

Ortho-hydroxybenzaldehydes reacted via Perkin condensation with the corresponding arylacetic acids and *N,N'*-dicyclohexylcarbodiimide (DCC) acting as dehydrating agent, to obtain compounds **1-3**, **5-14**, **16** and **17**. Afterwards, the ethoxy derivatives **3** and **14** gave the respective compounds **4** and **15**, by acidic hydrolysis in the presence of hydriodic acid (HI) 57%, acetic acid (AcOH) and acetic anhydride (Ac₂O).

Acetoxy-3-arylcoumarins **18-22** were prepared via Perkin-Oglialoro condensation. Following its traditional methodology, *ortho*-hydroxybenzaldehydes and arylacetic acids reacted for 16 h, at reflux temperature, in the presence of potassium acetate (CH₃CO₂K) and acetic anhydride (Ac₂O). Under these mild conditions, concomitant acetylation of the hydroxyls and closure of the pyrone ring occur. The hydrolysis of the acetoxy compounds was then carried out using aqueous hydrochloric acid (HCl) and methanol (MeOH), at

reflux temperature, for 3 h. This reaction allowed obtaining hydroxyl substituted 3-arylcoumarins **23-27**.

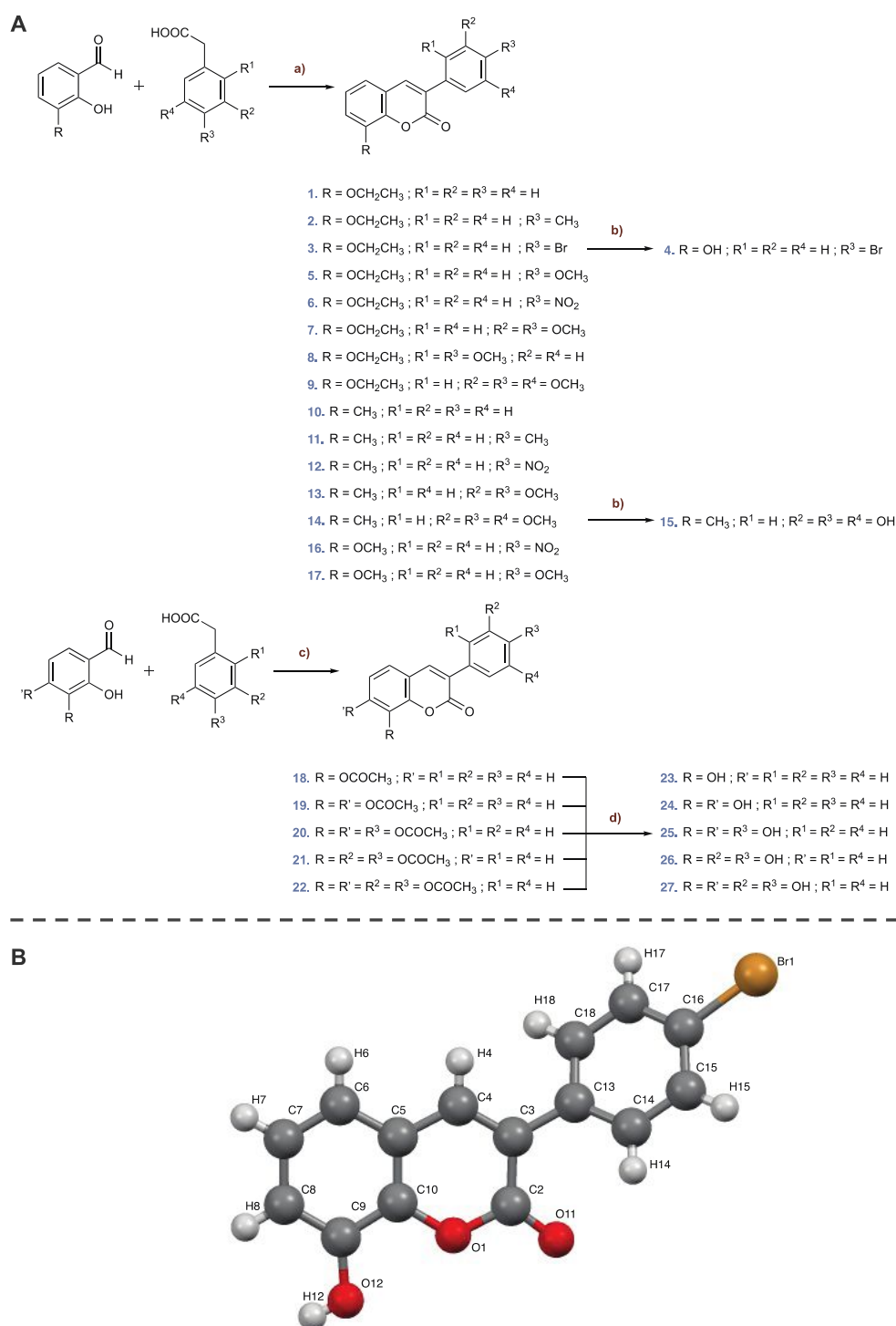


Figure 2. A. Scheme of the synthetic methodologies. a) DCC, DMSO, 110 °C, 24 h. b) HI, AcOH, Ac₂O, reflux, 3 h. c) CH₃CO₂K, Ac₂O, reflux, 16 h; d) HCl, MeOH, reflux, 3

h. **B.** Molecular structure of compound **4**, showing the atom-numbering scheme used in the X-ray study.

The structural analyses of compound **4** by X-ray crystallography (CCDC number 1937910)²⁶ corroborated the NMR information. This molecule is a coumarin derivative with a *p*-bromophenyl at position 3 of the coumarin and a hydroxyl at position 8, as represented in the scheme (Figure 2B). The dihedral angle formed by both planes of the 3-arylcoumarin scaffold ($\sim 36.6 \pm 2.1^\circ$) may reveal some important information on the possible binding pose of compound **4** to the receptor, being typical of these family of molecules.²⁷ In addition, the C3—C13 bond length is typical from the 3-arylcoumarins 1.483 Å. This length is coincident with the one reported for the 3-phenylcoumarin, crystalized by our research group.²⁷ Also, coumarin's planarity is corroborated by the torsion angles between its carbon atoms. Besides the interest in organic chemistry and structural elucidation, the deep structural knowledge of a molecule can be a significant tool for the understanding of its potential affinity and/or selectivity for particular receptors. All the details of the synthetic methodologies and characterization of the studied molecules are presented in the experimental section of this manuscript.

Pharmacological study. The affinity of the newly described coumarins for the A₁, A_{2A}, and A₃ adenosine receptors was evaluated using a protocol based on radioligand binding. A functional assay (inhibition of agonist-stimulated adenylyl cyclase activity) was performed to assess the affinity for the A_{2B} receptor.^{28,29} All the details are included in the experimental section. A₁, A_{2A} and A₃ adenosine receptors binding data is represented in Table 1. All the studied molecules became inactive against the A_{2B} receptor (IC₅₀ > 30 μM, data not shown).

Table 1. K_i values for the binding affinity of compounds **1-27** and reference compounds for human A₁, A_{2A} and A₃ receptors expressed in Chinese hamster ovary (CHO) cells.

Compound	R	R'	R ₁	R ₂	R ₃	R ₄	hA ₁ (μM)	hA _{2A} (μM)	hA ₃ (μM)
1	OCH ₂ CH ₃	-	H	H	H	H	22.1 (18.0-27.1)	55.0 (36.4-83.1)	22.5 (14.0-36.3)
2	OCH ₂ CH ₃	-	H	H	CH ₃	H	> 100	> 60	3.93 (2.57-6.01)
3	OCH ₂ CH ₃	-	H	H	Br	H	> 100	> 100	> 100
4	OH	-	H	H	Br	H	> 100	> 100	0.258 (0.143-0.468)
5	OCH ₂ CH ₃	-	H	H	OCH ₃	H	> 100	> 100	5.32 (3.68-7.68)
6	OCH ₂ CH ₃	-	H	H	NO ₂	H	> 100	> 100	> 100
7	OCH ₂ CH ₃	-	H	OCH ₃	OCH ₃	H	> 100	> 100	13.7 (9.55-19.6)
8	OCH ₂ CH ₃	-	OCH ₃	H	OCH ₃	H	> 100	> 100	16.6 (10.5-26.1)
9	OCH ₂ CH ₃	-	H	OCH ₃	OCH ₃	OCH ₃	> 100	> 100	9.05 (6.05-13.5)
10	CH ₃	-	H	H	H	H	14.8 (9.34-23.3)	42.1 (33.6-52.7)	17.0 (11.2-25.7)
11	CH ₃	-	H	H	CH ₃	H	> 100	> 100	16.6 (10.2-26.9)
12	CH ₃	-	H	H	NO ₂	H	> 100	> 100	> 100
13	CH ₃	-	H	H	OCH ₃	H	> 100	25.9 (17.7-38.0)	13.6 (12.3-15.2)
14	CH ₃	-	H	OCH ₃	OCH ₃	OCH ₃	> 60	32.9 (20.5-53.0)	9.82 (7.90-12.2)
15	CH ₃	-	H	OH	OH	OH	14.7 (8.74-24.6)	> 100	14.3 (7.79-26.4)

16	OCH ₃	-	H	H	NO ₂	H	> 100	59.1 (57.1-61.2)	8.02 (6.90-9.32)
17	OCH ₃	-	H	H	OCH ₃	H	> 100	> 100	5.06 (3.89-6.57)
18	OCOCH ₃	H	H	H	H	H	6.93 (5.76-8.33)	35.7 (27.9-45.8)	6.86 (5.86-8.03)
19	OCOCH ₃	OCOCH ₃	H	H	H	H	8.56 (6.90-10.6)	21.1 (16.6-26.8)	5.17 (4.85-5.50)
20	OCOCH ₃	OCOCH ₃	H	H	OCOCH ₃	H	> 100	> 100	6.14 (3.24-11.6)
21	OCOCH ₃	H	H	OCOCH ₃	OCOCH ₃	H	> 100	64.4 (49.0-84.6)	22.0 (12.5-38.7)
22	OCOCH ₃	OCOCH ₃	H	OCOCH ₃	OCOCH ₃	H	> 100	> 100	23.4 (14.5-37.9)
23	OH	H	H	H	H	H	4.62 (4.24-5.04)	42.3 (36.5-49.1)	5.09 (3.40-7.60)
24	OH	OH	H	H	H	H	2.40 (1.95-2.95)	12.1 (9.69-15.2)	3.85 (3.04-4.89)
25	OH	OH	H	H	OH	H	12.5 (10.3-15.4)	55.3 (45.3-67.4)	9.16 (7.12-11.8)
26	OH	H	H	OH	OH	H	6.20 (5.11-7.53)	14.0 (10.1-19.5)	23.6 (16.8-33.2)
27	OH	OH	H	OH	OH	H	6.28 (5.26-7.49)	25.5 (21.2-30.5)	8.50 (7.47-9.67)
Theophylline			-				6.77 (4.07-11.3)	1.71 (1.02-2.90)	86.4 (73.6-101)

Values are geometric means of three experiments and are given in μM with 95% confidence intervals. Numbers in brackets are the numerical value of the standard uncertainty.

Based on previous results from our group, and on the potent A₃ receptor affinity of some of the described compounds,²¹ a novel family of coumarin-containing compounds was investigated. Their specific framework formed by an aryl ring attached to position 3 and a substitution pattern at positions 7 and/or 8 was analyzed for their capability to modulate

the affinity for adenosine receptor subtypes. Different chemical features were attached to the phenyl ring at position 3, based on their physicochemical properties. Substituents from different quadrants of the Craig plot were explored. In addition, the substitution by alkyl or alkoxy groups was studied. Finally, the difference between the presence of acetoxy and/or hydroxy substituents at 7 and/or 8 positions of the coumarin scaffold was explored in detail. The effect of these substitutions on the binding and the level of selectivity for the receptors was studied and compared. From our analysis, no affinity for the A_{2B} receptor was observed ($K_i > 30 \mu\text{M}$, data not shown).

The structural variety on the studied series allowed us to obtain different affinity profiles for the analyzed adenosine receptors. Selective A₃ ligands, A_{2A}/A₃ or A₁/A₃ dual ligands or non-selective (A₁/A_{2A}/A₃) ligands were obtained. The analysis of the results allowed us to have a detailed perspective on structure-activity relationships. In general, compounds without attached groups on the 3-phenyl moiety are not selective, presenting affinity for the three adenosine receptors (compounds **1**, **10**, **18**, **19**, **23** and **24**). This profile is independent of the nature of the 8 substitution (ethoxy, methyl, acetoxy) or even with substitutions at both 7 and 8 positions (compound **19**). These results are accordant with those obtained in our previous study.²¹ 8-(2-Oxopropoxy)-3-phenylcoumarin (Figure 1A) has reported affinity for three of the studied receptors in the low micromolar range (K_i A₁ = 10.4 μM , K_i A_{2A} = 16.1 μM and K_i A₃ = 7.1 μM).²¹ In the present study, compound **24** shows similar affinity for the three adenosine receptors (K_i A₁ = 2.4 μM , K_i A_{2A} = 12.1 μM and K_i A₃ = 3.9 μM). In addition, compound **24** proved to be a better adenosine receptor ligand than theophylline, our reference compound, which is in clinical use to prevent and treat respiratory dysfunctions caused by asthma, emphysema, chronic bronchitis, and other lung diseases.³⁰ Besides being an A_{2B} receptor antagonist, theophylline is also a non-selective phosphodiesterase inhibitor. The profile of our

1
2
3 $A_1/A_{2A}/A_3$ compounds may be very interesting thinking about multifactorial conditions,
4
5 as lung ischemia-reperfusion injury, likewise some xanthines, typical adenosine ligands.

6
7 When the scaffold presents a substituent at position 8 and another one at *para* position of
8
9 the 3-aryl moiety, independently of the nature of the substituent at positions 8 (ethoxy,
10
11 hydroxy, methyl or methoxy) or 3 (*p*-methylphenyl, *p*-bromophenyl or *p*-
12
13 methoxyphenyl), the compounds tend to be strong and selective A_3 ligands (compounds
14
15 **2**, **4**, **11** and **17**). This data expands our previously results.²¹ The nanomolar affinity of
16
17 compound **4** for the hA_3 receptor is about 2.5 times higher than that of our earlier reported
18
19 8-(2-oxopropoxy)-3-(*p*-tolyl)coumarin (Figure 1A).²¹ So far, this is the best compound
20
21 from all our research on the potential of coumarins as adenosine receptor ligands. In both
22
23 cases, position 8 presents electron donating groups. This characteristic can be important
24
25 to increase the activity and A_3 selectivity. In addition, it seems that the size of the
26
27 atom/group at position 8 plays an important role on the activity as well.

28
29 Another relevant relationship between the structure and the measured activity was
30
31 observed for the series presenting 2- or 3-substitutions at the 3-aryl ring (*meta* and *para*
32
33 positions). Compounds **13**, **14** and **21** have affinity for both A_{2A} and A_3 , and compound
34
35 **15** has affinity for A_1 and A_3 receptors. The only example of a di-substituted compound
36
37 at *ortho/para* positions (compound **8**), proved to be A_3 receptor selective ($K_i A_3 = 16.6$
38
39 μM).

40
41 Finally, the inclusion of substituents at both 7 and 8 positions of the coumarin ring (both
42
43 acetoxy and hydroxy groups), independently of the substituents on the 3-aryl ring, tend
44
45 to give potent non-selective ligands (compounds **19**, **24**, **25** and **27**). All these compounds
46
47 have affinity for the A_1 , A_{2A} and A_3 adenosine receptors in the low micromolar range.
48
49 Compounds **20** and **22** are the exception, being selective for the A_3 receptor.
50
51

52
53 Finally, our most active and selective hA_3 compounds were functionally tested using the
54
55
56
57
58
59
60

GloSensor cAMP assay, which consists in a biosensor technology.³¹ The methodology is detailed in the experimental section, and the binding information is shown in Table 2.

Table 2. *In vitro* antagonist activities of **2**, **4**, **5** and **17** at the hA₃ adenosine receptor.

Compound	hA ₃ (IC ₅₀ μM)
2	18.4 (10.5-26.2)
4	3.1 (1.7-4.5)
5	29.5 (17.7-41.2)
17	25.3 (15.5-31.1)

The values are given in μM with 95% confidence intervals in parentheses.

Cell-based functional assays showed that compounds **2**, **4**, **5** and **17** behave as hA₃ receptor antagonists, being able to counteract NECA-inhibited cAMP accumulation.

In a homogeneous family of twenty-seven compounds, it can be clearly observed a pattern of affinity based on the structures (positions and nature of the substituents) that allows new structure-affinity relationship understanding.

Molecular docking

We studied the most active molecule within the designed family using docking calculations in the hA₃ receptor to establish the key residues and important interactions between the ligand and the protein. Our research group previously generated the hA₃ protein structure by homology modeling (general details are described in Methods).^{21,32} We docked compound **4** to the hA₃ with Glide standard precision (SP).³³ We followed a

similar protocol already described in previous studies^{21,32} and validated in the hA_{2A} protein for which there are some crystal structures available in the PDB. As an example, the root mean square deviation (RMSD) comparing ligands theoretical with co-crystallized conformations in the 3EML³⁴ and 3UZC crystal structures³⁵ was 0.69 and 1.90.²¹

Molecular docking simulations presented a binding pose for compound **4** in the hA₃ pocket that pointed the 3-aryl portion towards the bottom and the benzene of the coumarin towards the surface (see Figure 3A). Compound **4** showed a pose in the hA₃ that presented some resemblance with the co-crystallized ligands ZM241385 and T4E in the 3EML and 3UZC hA_{2A} crystal structures (see Figure 3B). The hydroxyl substituent at position 8 along with the carbonyl group are hypothesized to be important for the anchoring with the studied protein and established two hydrogen bonds with the residue Asn250, interacting via its amide (see Figure 3C). The equivalent residue in the hA_{2A} (Asn253) showed also an important role in ligand interaction in crystallographic and mutagenesis studies.^{34,35,36} The benzopyrone moiety is proposed to establish aromatic π - π stacking interactions with Phe168 residue of the second extracellular loop.

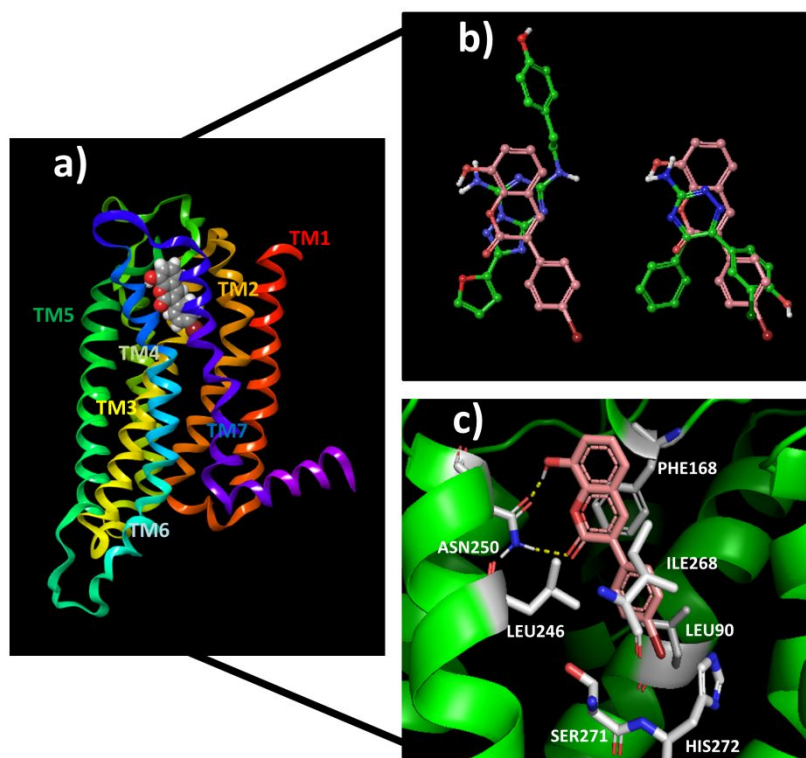


Figure 3. a) General view of the hA₃ receptor bound to compound 4. b) Comparison of the co-crystallized conformations for the compounds (carbons in green) in the hA_{2A} [3EML (left) and 3UZC (right)] with the binding mode observed by docking in hA₃ for compound 4 (pink carbons). Both proteins, hA_{2A} and hA₃, were superimposed. c) Hypothetical binding mode in the hA₃ determined for compound 4 along with relevant residues in ligand interaction. Hydrogen bonds are colored in yellow. For clarity, protein ribbons were partially omitted. Template for the hA₃ homology model: 3EML.

We extended the ligand-protein interaction analysis to per residue energy contributions (see Figure 4A). The total energy is obtained from different contributions considering Coulomb, *van der Waals* and H-bond energies. Residues Asn250, Phe168, Ile268, Leu246, Leu264 and Leu90 have the highest contribution in the ligand-protein recognition. Hydroxyl group at position 8 seems to be important for the interaction with

residue Asn250 and it could be the explanation for the high activity displayed by compound **4**. The bromine substituent at *para* position of the 3-aryl moiety could be also a suitable substituent for the protein interaction. Compound **23**, structurally similar to compound **4** but with no substitution in the 3-aryl ring showed a similar binding mode, but with lower Coulomb/*van der Waals* contributions with the residues close to the 3-aryl (see Figure 4B). The bromine substituent caused a slight increase in the interaction with residues Leu90, Ser271 and His272 compared to the 3-aryl ring without substituent (compound **23**). Moreover, we calculated the favored hydrophobic and hydrophilic areas inside the hA₃ protein pocket. The surfaces were generated taking into account the residues located in a radius of 5Å from the ligand. The hydroxyl substituent presented at 8 position of the coumarin system and the oxygen atoms part of the pyrone system are placed in polar areas whereas the coumarin and the 3-aryl scaffold are placed in a hydrophobic area (Figure 4C). The bromine atom is buried in a deep hydrophobic area that can favor the interaction with the protein. In fact, besides hydrophobic interactions with residues Trp243 and Leu90 (also shown by compound **23**) we detected additional hydrophobic interactions with residues Val65 and Val61. The bromine atom does not interact through halogen bonds with the protein, but its hydrophobic nature is well suited for the hydrophobic surrounding residues. Our proposed binding mode explains the high affinity of compound **4** for hA₃ receptor. Our results agree with previous studies focused on adenosine receptors^{21,32,34-37} in which residues as Asn250 and Phe168 were also reported as important in ligand-protein recognition.

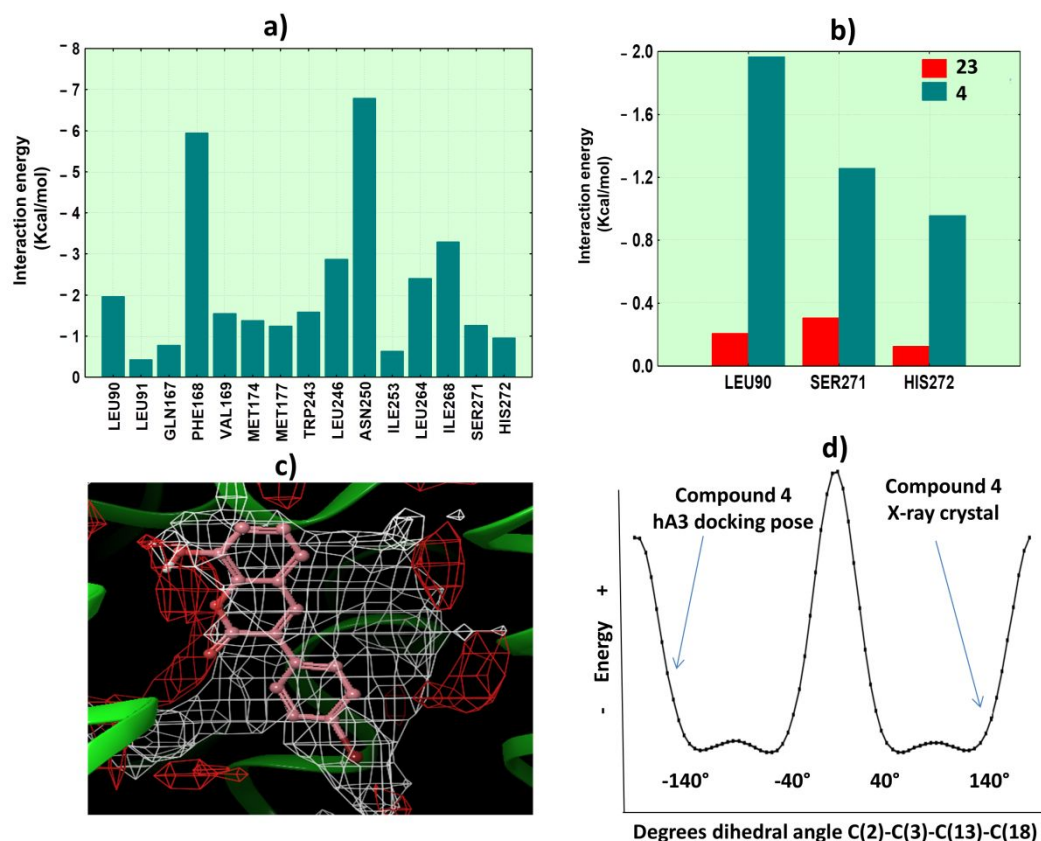


Figure 4. **a)** Residue contribution to the interaction with ligand **4** (including *van der Waals*, Coulomb and hydrogen bond energies). **b)** Differences in the residue contribution of compounds **4** and **23**. Bromine substitution in the 3-aryl ring (compound **4**) causes a higher Coulomb/*van der Waals* contribution in nearby residues. **c)** Hydrophobic (white) and hydrophilic (red) areas inside the hA₃ with the binding mode detected for compound **4** (isovalues of -0.5 and -4.87 for hydrophobic and hydrophilic surfaces respectively). The 8-hydroxyl is placed in the hydrophilic area while the 3-aryl scaffold is placed in the hydrophobic one (template for the hA₃ homology model: 3EML). **d)** Dihedral angle energy plot for compound **4** extracted from conformational analysis.

The results provided by the docking calculations are aligned with the X-ray structure of compound **4** (RMSD=0.16Å). As the analysis of the conformational preorganization of the compound could provide some insights in drug design,³⁸ we performed a comparative

structural study in terms of energetic stabilization around the dihedral angle C(2)-C(3)-C(13)-C(18) between the 3-aryl ring and the coumarin scaffold in compound **4**. The dihedral angle was rotated in 5-degree increments during the conformational analysis. Compound **4** showed two optimal energetic areas with values for the dihedral angle from -140° to -40° and from 40° to 140°. The described X-ray crystallized structure and the docking pose showed values of 145.4° and -152.1° for the dihedral angle. It has been reported that in many cases the bioactive ligand conformation is not correspondent with the global minimum energy conformer as both protein and ligand can reorganize their atomic coordinates to optimize complementarity.³⁹ For compound **4**, the X-ray and the docking conformation are close to the global minimum energy structure. The dihedral angle energy plot for compound **4** is shown in Figure 4D with the values obtained in docking and X-ray studies.

Compound **4** showed hA₃ activity and no affinity for the other adenosine subtypes. We performed additional molecular docking simulations in the hA_{2A} crystallized structure 3EML to explain the affinity decrease for compound **4**. Molecular docking with no crystallographic water molecules in the hA_{2A} binding region yielded a binding mode deeply buried in the cavity (see Figure 5A). The displacement of water in the pocket could have a positive or negative impact in ligand binding affinity and enthalpy/entropy of the system.⁴⁰ The 4-bromophenyl scaffold of compound **4** with hydrophobic characteristics is placed in the polar area occupied by the water in the hA_{2A}. This scaffold has not the potential to establish similar hydrogen bonds to the hydrogen bonding network described by the water molecules. As a hypothesis, the global process could be energetically unfavorable reducing the activity of compound **4** in hA_{2A}. Nevertheless, the docking with crystallographic water molecules in the hA_{2A} cavity showed a pose for compound **4** that binds a shallower area of the pocket and disrupts key interactions with some residues

located deeper in the cavity, such as Asn253 (see Figure 5B). The disruption of the binding mode explained for compound **4** in the hA₃ could be responsible for the low activity detected in hA_{2A}. In fact, compound **4** showed a different residue profile binding in the hA₃ and hA_{2A} with a clear reduction in the interaction energy between the ligand and Asn253, a key residue in the interaction between compound **4** and the hA₃ (see Supporting Information).

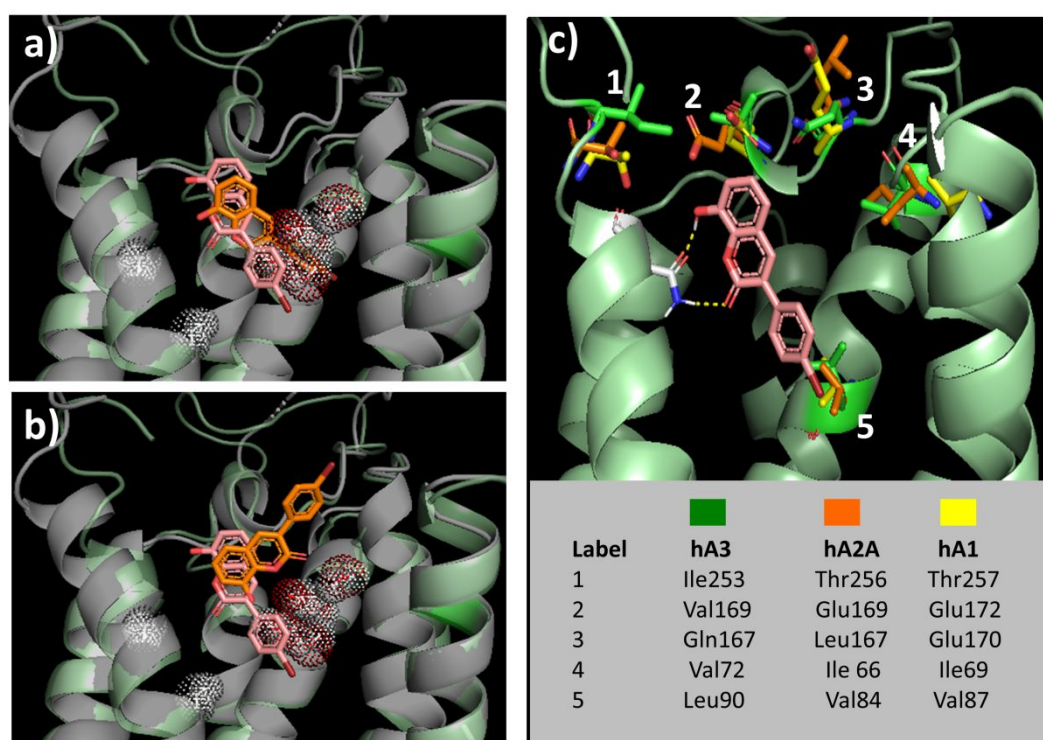


Figure 5. Superposition of the binding poses for compound **4** observed by docking in hA₃ (ligand in pink carbons) and hA_{2A} (ligand in orange carbons). **a)** Hypothetical binding mode of compound **4** buried in an area of multiple crystallographic water molecules in the hA_{2A} (although water molecules are shown in red/white mesh, the docking was performed with no water in the cavity). This hypothetical pose would need to displace the mentioned waters. **b)** Hypothetical binding mode of compound **4** in a shallower area close to the extracellular loops in the hA_{2A} (docking performed considering the water molecules

presented in the protein pocket). Disruption of the binding mode detected for compound **4** in hA₃ (carbons in pink) could be the cause of lack of affinity in the hA_{2A}. c) Key residues in ligand recognition in the hA₃ that are not conserved in both hA_{2A} and hA₁ subtypes. Other residues that differ in the hA₃, hA_{2A} and hA₁ subtypes are Leu264, Met270 and Thr270 respectively, not represented in the figure due to clarity reasons.

The residue Leu90 in the hA₃ that established key interactions with the 4-bromophenyl of compound **4** is substituted by Val84 and Val87 in the hA_{2A} and hA₁ respectively, although those residues present similar hydrophobic characteristics. However, some of the residues located in the extracellular domain of the hA₃ are not present in the other subtypes, which can be also an important factor to explain the selectivity. Residues such as Gln167 with polar properties, Val169, Ile253 and Leu264 with hydrophobic characteristics are substituted in the hA_{2A} by the corresponding hydrophobic Leu167, the negative charged and hydrophilic Glu169, Thr256 with hydrophilic properties and the hydrophobic Met270. The subtype hA₁ contains some residues, as Glu170, Glu172, Thr270 and Thr257 with hydrophilic properties more suitable for the interaction with polar substituents. Figure 5C shows important residues in ligand recognition in the hA₃ that are not conserved in both hA_{2A} and hA₁ subtypes. The chemical characteristics of the residues can affect the entrance of the designed ligand in the pocket as well as the accommodation in the binding cleft and favor the selectivity against the hA₃.

Conclusions

3-Arylcoumarins proved to be an attractive scaffold for the development of multitarget molecules. In particular, 8-substituted compounds are promising molecules as novel antagonists of adenosine receptors, presenting different affinity and selectivity profiles.

An extensive overview of our experimental data helped to conclude that both affinity and/or selectivity profiles of the new molecules against adenosine receptors could be modified taking into account the characteristics of the substituents at positions 3, 7 and 8 of the coumarins. Compound **4** (3-(4-bromophenyl)-8-hydroxycoumarin) appeared as the best compound within this study, and all the molecules developed by our group so far. Its structure was corroborated by X-ray crystallography, revealing that this coumarin derivative presents a *p*-bromophenyl substituent at 3 position, presenting a hydroxyl group attached to position 8 as well. This last substituent proved to be fundamental for the interaction with Asn250 residue and it could be the answer to explain the high affinity showed by this antagonist. The substituents on the 3-aryl ring are also important for this selectivity pattern. On the other hand, compound **24** proved to display the highest affinity on three receptors, being a better ligand than the reference compound, theophylline. This series offers the possibility to better understand important clues to modulate the interactions with adenosine receptors. Compound **24** can be the inspiration for the design of multifunctional compounds with interest on multifactorial conditions, and compound **4** can be the inspiration for the development of new coumarins as strong and selective A₃ antagonists.

EXPERIMENTAL SECTION

CHEMISTRY

General remarks. Starting materials and reagents were obtained from commercial suppliers (Sigma-Aldrich) and were used without further purification. Melting points (Mp) are uncorrected and were determined with a Reichert Kofler thermopan or in capillary tubes in a Büchi 510 apparatus. ¹H NMR (300 MHz) and ¹³C NMR (75.4 MHz) spectra were recorded with a Bruker AMX spectrometer using CDCl₃ or DMSO-*d*₆ as

solvent. Chemical shifts (δ) are expressed in parts per million (ppm) using TMS as an internal standard. Coupling constants J are expressed in Hertz (Hz). Spin multiplicities are given as s (singlet), d (doublet), t (triplet), q (quartet) and m (multiplet). Mass spectrometry was carried out with a Hewlett-Packard 5988A spectrometer. Elemental analyses were performed by a Perkin-Elmer 240B microanalyzer and are within $\pm 0.4\%$ of calculated values in all cases. The analytical results document $\geq 98\%$ purity for all compounds. Flash chromatography (FC) was performed on silica gel (Merck 60, 230-400 mesh); analytical TLC was performed on precoated silica gel plates (Merck 60 F254). Organic solutions were dried over anhydrous sodium sulfate. Concentration and evaporation of the solvent after reaction or extraction was carried out on a rotary evaporator (Büchi Rotavapor) operating under reduced pressure.

General procedure for the synthesis of 3-phenylcoumarins (1-3, 5-14, 16 and 17). A solution of 2-hydroxybenzaldehyde (7.34 mmol) and the corresponding phenylacetic acid (9.18 mmol) in dimethyl sulfoxide (15 mL) was prepared. *N,N'*-Dicyclohexylcarbodiimide (11.46 mmol) was added, and the mixture was heated in an oil bath at 110 °C for 24 h. Ice (100 mL) and acetic acid (10 mL) were added to the reaction mixture. After keeping it at room temperature for 2 h, the mixture was extracted with ether (3 x 25 mL). The organic layer was extracted with sodium bicarbonate solution (50 mL, 5%) and then water (20 mL). The solvent was evaporated under vacuum, and the dry residue was purified by FC (hexane/ethyl acetate 9:1).

General procedure for the synthesis of hydroxy-3-phenylcoumarins (4 and 15). A solution of **3** or **14** (0.50 mmol) in acetic acid (5 mL) and acetic anhydride (5 mL), at 0 °C, was prepared. Hydriodic acid 57% (10 mL) was added dropwise. The mixture was

1
2
3 stirred, under reflux temperature, for 3 h. The solvent was evaporated under vacuum, and
4
5 the dry residue was purified by crystallization (CH₃CN).
6

7
8 **General procedure for the synthesis of acetoxy-3-phenylcoumarins (18-22).**
9

10 Compound **18-22** were synthesized under anhydrous conditions, using material
11 previously dried at 60 °C for at least 12 h and at 300 °C during few minutes immediately
12 before use. A solution containing anhydrous CH₃CO₂K (2.94 mmol), phenylacetic acid
13 (1.67 mmol) and the corresponding hydroxysalicylaldehyde (1.67 mmol), in Ac₂O (1.2
14 mL), was refluxed for 16 h. The reaction mixture was cooled, neutralized with 10%
15 aqueous NaHCO₃, and extracted with EtOAc (3 x 30 mL). The organic layers were
16 combined, washed with distilled water, dried (anhydrous Na₂SO₄), and evaporated under
17 reduced pressure. The product was purified by recrystallization in EtOH and dried, to
18 afford the desired compound.
19
20
21
22
23
24
25
26
27
28
29

30
31 **General procedure for the synthesis of hydroxy-3-phenylcoumarins (23-27).**
32

33 Compounds **23-27** were obtained by hydrolysis of their acetoxyated counterparts **18-22**,
34 respectively. The appropriate acetoxyated coumarin, mixed with 2N aqueous HCl and
35 MeOH, was refluxed during 3 h. The resulting reaction mixture was cooled in an ice-bath
36 and the reaction product, obtained as solid, was filtered, washed with cold distilled water,
37 and dried under vacuum, to afford the desired compound.
38
39
40
41
42
43
44
45
46

47 **3-(4-bromophenyl)-8-ethoxycoumarin (compound 3).** Yield 41%. M.p. 162-163 °C. ¹H
48 NMR (CDCl₃) δ (ppm), *J* (Hz): 1.52 (t, 3H, CH₃, *J*=7.0), 4.20 (q, 2H, CH₂, *J*=7.0), 7.06-
49 7.24 (m, 3H, H-5, H-6, H-7), 7.32-7.45 (m, 4H, H-2', H-3', H-5', H-6'), 7.79 (s, 1H, H-
50 4). ¹³C NMR (CDCl₃) δ (ppm): 14.8, 65.0, 114.7, 119.3, 120.2, 123.14 124.5, 127.3,
51 130.1, 131.6, 133.6, 140.2, 143.4, 146.4, 159.9. MS *m/z* (%): 347 (18), 346 (98), 345 (19),
52
53
54
55
56
57
58
59
60

344 (M^+ , 100). Ana. Elem. Calc. for $C_{17}H_{13}BrO_3$: C, 59.15; H, 3.80. Found: C 58.98, H 3.80.

3-(4-bromophenyl)-8-hydroxycoumarin (compound 4). Yield 42%. M.p. 261-217 °C.

1H NMR ($DMSO-d_6$) δ (ppm), J (Hz): 7.05-7.16 (m, 3H, H-5, H-6, H-7), 7.56-7.71 (m, 4H, H-2', H-3', H-5', H-6'), 8.22 (s, 1H, H-4), 10.27 (s, 1H, OH). ^{13}C NMR ($DMSO-d_6$) δ (ppm): 118.2, 118.7, 120.3, 121.9, 124.6, 125.5, 130.6, 131.2, 133.9, 141.3, 141.7, 144.4, 159.5. MS m/z (%): 319 (16), 318 (98), 317 (17), 316 (M^+ , 100). Ana. Elem. Calc. for $C_{15}H_9BrO_3$: C, 56.81; H, 2.86. Found: C 56.84, H 2.87.

8-ethoxy-3-(3,4-dimethoxyphenyl)coumarin (compound 7). Yield 41%. M.p. 138-139

°C. 1H NMR ($CDCl_3$) δ (ppm), J (Hz): 1.53 (t, 3H, CH_3 , $J=7.0$), 3.90 (s, 3H, OCH_3), 3.95 (s, 3H, OCH_3), 4.21 (q, 2H, CH_2 , $J=7.0$), 6.94 (d, 1H, H-7, $J=8.2$), 7.02-7.09 (m, 2H, H-2', H-6'), 7.20 (d, 1H, H-5', $J=7.9$), 7.28-7.33 (m, 2H, H-5, H-6), 7.77 (s, 1H, H-4). ^{13}C NMR ($CDCl_3$) δ (ppm): 14.5, 55.7, 64.6, 110.7, 111.5, 114.0, 118.9, 120.2, 121.0, 124.0, 127.1, 128.0, 138.7, 142.8, 146.0, 148.4, 149.4, 160.1. MS m/z (%): 327 (55), 326 (M^+ , 100). Anal. Elem. Calc. for $C_{19}H_{18}O_5$: C, 69.93; H, 5.56. Found: C, 69.91; H, 5.53.

8-ethoxy-3-(2,4-dimethoxyphenyl)coumarin (compound 8). Yield 36%. M.p. 95-96

°C. 1H NMR ($CDCl_3$) δ (ppm), J (Hz): 1.50 (t, 3H, CH_3 , $J=7.0$), 3.80 (s, 3H, OCH_3), 3.82 (s, 3H, OCH_3), 4.19 (q, 2H, CH_2 , $J=7.0$), 6.45-6.57 (m, 2H, H-3', H-5'), 7.03-7.09 (m, 1H, H-7), 7.14-7.19 (m, 2H, H-6, H-5), 7.30 (d, 1H, H-6', $J=8.9$), 7.68 (s, 1H, H-4). ^{13}C NMR ($CDCl_3$) δ (ppm): 14.8, 55.4, 55.7, 64.9, 99.0, 104.5, 114.1, 116.8, 119.1, 120.4, 124.0, 126.3, 131.4, 141.4, 146.3, 154.2, 158.3, 160.2, 161.4. MS m/z (%): 327 (12), 326 (M^+ , 47). Anal. Elem. Calc. for $C_{19}H_{18}O_5$: C, 69.93; H, 5.56. Found: C, 69.96; H, 5.58.

8-ethoxy-3-(3,4,5-trimethoxyphenyl)coumarin (compound 9). Yield 40%. M.p. 142-

143 °C. 1H NMR ($CDCl_3$) δ (ppm), J (Hz): 1.58 (t, 3H, CH_3 , $J=7.0$), 3.94 (s, 3H, OCH_3), 3.96 (s, 3H, OCH_3), 3.99 (s, 3H, OCH_3), 4.25 (q, 2H, CH_2 , $J=7.0$), 7.0 (s, 2H, H-2', H-

6'), 7.14-7.20 (m, 1H, H-6), 7.24-7.27 (m, 1H, H-7), 7.30-7.32 (m, 1H, H-5), 7.83 (s, 1H, H-4). ^{13}C NMR (CDCl_3) δ (ppm): 14.8, 56.2, 56.3, 65.0, 105.9, 114.5, 119.2, 120.3, 124.4, 128.2, 130.2, 139.7, 133.8, 146.3, 153.0. MS m/z (%): 357 (23), 356 (M^+ , 100). Anal. Elem. Calc. for $\text{C}_{20}\text{H}_{20}\text{O}_6$: C, 67.41; H, 5.66. Found: C, 67.42; H, 5.68.

8-methyl-3-(4-nitrophenyl)coumarin (compound 12). Yield 61%. M.p. 229-230 °C. ^1H NMR ($\text{DMSO}-d_6$) δ (ppm), J (Hz): 2.38 (s, 3H, CH_3), 7.28 (t, 1H, H-6, $J=7.4$), 7.52 (d, 1H, H-7, $J=7.4$), 7.61 (d, 1H, H-5, $J=7.4$), 7.99 (d, 2H, H-2', H-6', $J=9.0$), 8.28 (d, 2H, H-3', H-5', $J=9.0$), 8.41 (s, 1H, H-4). ^{13}C NMR ($\text{DMSO}-d_6$) δ (ppm): 15.3, 123.8, 124.8, 124.9, 125.4, 127.3, 130.2, 131.3, 134.1, 141.8, 143.4, 147.5, 152.0, 159.8. MS m/z (%): 282 (18), 281 (M^+ , 100). Anal. Elem. Calc. for $\text{C}_{16}\text{H}_{11}\text{NO}_4$: C, 68.33; H, 3.94. Found: C, 68.36; H, 3.93.

3-(3,4-dimethoxyphenyl)-8-methylcoumarin (compound 13). Yield 63%. M.p. 135-136 °C. ^1H NMR (CDCl_3) δ (ppm), J (Hz): 2.51 (s, 3H, CH_3), 3.94 (s, 6H, $2\times\text{OCH}_3$), 6.95 (d, 1H, H-5', $J=8.1$), 7.16-7.39 (m, 5H, H-5, H-6, H-7, H-2', H-6'), 7.77 (s, 1H, H-4). ^{13}C NMR (CDCl_3) δ (ppm): 15.4, 55.9, 110.9, 111.7, 119.4, 121.1, 124.0, 125.4, 125.8, 127.5, 127.5, 132.4, 139.2, 148.6, 149.6, 151.6, 160.9. MS m/z (%): 297 (46), 296 (M^+ , 100). Anal. Elem. Calc. for $\text{C}_{18}\text{H}_{16}\text{O}_4$: C, 72.96; H, 5.44. Found: C, 73.00; H, 5.49.

3-(3,4,5-trimethoxyphenyl)-8-methylcoumarin (compound 14). Yield 69%. M.p. 163-164 °C. ^1H NMR (CDCl_3) δ (ppm), J (Hz): 2.49 (s, 3H, CH_3), 3.89 (s, 3H, OCH_3), 3.90 (s, 3H, OCH_3), 3.93 (s, 3H, OCH_3), 6.95 (s, 2H, H-2', H-6'), 7.18-7.23 (m, 2H, H-6, H-7), 7.38 (d, 1H, H-5, $J=7.4$), 7.79 (s, 1H, H-4). ^{13}C NMR (CDCl_3) δ (ppm): 15.4, 56.2, 56.3, 106.0, 119.3, 124.1, 125.6, 125.9, 127.7, 130.3, 132.7, 138.7, 139.9, 151.7, 153.1, 160.7. MS m/z (%): 327 (23), 326 (M^+ , 100). Ana. Elem. Calc. for $\text{C}_{19}\text{H}_{18}\text{O}_5$: C, 69.93; H, 5.56. Found: C, 69.96; H, 5.59.

8-acetoxy-3-phenylcoumarin (compound 18). Yield 64%. M.p. 189-190 °C. ¹H NMR (CDCl₃) δ (ppm), *J* (Hz): 2.44 (s, 3H, CH₃), 7.18-7.50 (m, 7H, H-2', H-3', H-4', H-5', H-6', H-6, H-7), 7.66-7.71 (m, 1H, H-5), 7.83 (s, 1H, H-4). ¹³C NMR (CDCl₃) δ (ppm): 20.7, 119.3, 123.0, 124.5, 124.8, 126.0, 128.2, 128.9, 129.2, 135.3, 142.1, 144.2, 149.2, 160.9, 168.5. MS *m/z* (%): 281 (19), 280 (M⁺, 100). Ana. Elem. Calc. for C₁₇H₁₂O₄: C, 72.85; H, 4.32. Found: C, 72.90; H, 4.30.

7,8-diacetoxy-3-phenylcoumarin (compound 19). Yield 81%. M.p. 171-172 °C. ¹H NMR (CDCl₃) δ (ppm), *J* (Hz): 2.34 (s, 3H, CH₃), 2.43 (s, 3H, CH₃), 7.15 (d, 1H, H-6, *J*=8.7), 7.39-7.49 (m, 4H, H-5, H-2', H-4', H-6'), 7.64-7.69 (m 2H, H-3', H-5'), 7.78 (s, 1H, H-4). ¹³C NMR (CDCl₃) δ (ppm): 20.3, 20.6, 118.5, 119.1, 124.9, 128.1, 128.5, 129.0, 130.0, 134.3, 139.1, 144.9, 146.5, 159.0, 167.4, 167.8. MS *m/z* (%): 339 (11), 338 (M⁺, 100). Ana. Elem. Calc. for C₁₉H₁₄O₆: C, 67.45; H, 4.17. Found: C, 67.52; H, 4.20.

7,8-diacetoxy-3-(4-acetoxyphenyl)coumarin (compound 20). Yield 75%. M.p. 195-196 °C. ¹H NMR (CDCl₃) δ (ppm), *J* (Hz): 2.32 (s, 3H, CH₃), 2.34 (s, 3H, CH₃), 2.42 (s, 3H, CH₃), 7.13-7.19 (m, 3H, H-6, H-3', H-5'), 7.41 (d, 1H, H-5, *J*=8.7), 7.68 (d, 2H, H-2', H-6', *J*=8.6), 7.77 (s, 1H, H-4). ¹³C NMR (CDCl₃) δ (ppm): 20.2, 20.5, 21.1, 118.3, 119.1, 121.6, 124.9, 127.1, 129.6, 131.8, 131.9, 139.1, 144.2, 144.92, 151.1, 161.9, 167.3. MS *m/z* (%): 397 (9), 396 (M⁺, 93). Ana. Elem. Calc. for C₂₁H₁₆O₈: C, 63.64; H, 4.07. Found: C, 63.61; H, 4.09.

8-acetoxy-3-(3,4-diacetoxyphenyl)coumarin (compound 21). Yield 47%. M.p. 144-145 °C. ¹H NMR (CDCl₃) δ (ppm), *J* (Hz): 2.33 (s, 6H, 2xCH₃), 2.44 (s, 3H, CH₃), 7.27-7.31 (m, 3H, H-5', H-2', H-6), 7.41-7.45 (m, 1H, H-7), 7.58-7.64 (m, 2H, H-6', H-5), 7.84 (s, 1H, H-4). ¹³C NMR (CDCl₃) δ (ppm): 20.6, 20.6, 20.6, 120.6, 123.4, 123.6, 124.3, 125.1, 125.4, 126.6, 127.0, 132.8, 137.5, 139.8, 139.9, 140.0, 141.9, 158.8, 168.0, 168.1,

168.5. MS m/z (%): 397 (15), 396 (M^+ , 89). Ana. Elem. Calc. for $C_{21}H_{16}O_8$: C, 63.64; H, 4.07. Found: C, 63.66; H, 4.10.

7,8-diacetoxy-3-(3,4-diacetoxyphenyl)coumarin (compound 22). Yield 54%. M.p. 202-203 °C. 1H NMR ($CDCl_3$) δ (ppm), J (Hz): 2.35 (s, 3H, CH_3), 2.37 (s, 3H, CH_3), 2.39 (s, 3H, CH_3), 2.46 (s, 3H, CH_3), 7.20 (d, 1H, H-6', $J=8.6$), 7.30 (s, 1H, H-2'), 7.46 (d, 1H, H-5', $J=8.6$), 7.59-7.65 (m, 2H, H-5, H-6), 7.84 (s, 1H, H-4). ^{13}C NMR ($CDCl_3$) δ (ppm): 20.1, 20.2, 20.5, 20.6, 118.1, 119.2, 122.0, 123.4, 123.6, 125.9, 126.2, 132.7, 139.5, 141.9, 142.6, 145.1, 148.9, 150.3, 160.4, 167.6. MS m/z (%): 455 (9), 454 (M^+ , 92). Ana. Elem. Calc. for $C_{23}H_{18}O_{10}$: C, 60.80; H, 3.99. Found: C, 60.82; H, 4.01.

7,8-dihydroxy-3-(4-hydroxyphenyl)coumarin (compound 25). Yield 91%. M.p. 290-291 °C. 1H NMR ($DMSO-d_6$) δ (ppm), J (Hz): 6.78-6.81 (m, 3H, H-6, H-3', H-5'), 7.04 (d, 1H, H-5, $J=8.5$), 7.51-7.55 (m, 2H, H-2', H-6'), 7.97 (s, 1H, H-4), 9.63 (s, 1H, OH), 10.05 (s, 1H, OH), 10.08 (s, 1H, OH). ^{13}C NMR ($DMSO-d_6$) δ (ppm): 115.0, 115.2, 116.3, 126.0, 126.6, 129.8, 133.6, 139.7, 142.5, 149.0, 149.3, 157.2, 162.7. MS m/z (%): 271 (16), 270 (M^+ , 100). Ana. Elem. Calc. for $C_{15}H_{10}O_5$: C, 66.67; H, 3.73. Found: C, 66.65; H, 3.75.

8-hydroxy-3-(3,4-dihydroxyphenyl)coumarin (compound 26). Yield 79%. M.p. 259-260 °C. 1H NMR ($DMSO-d_6$) δ (ppm), J (Hz): 7.79 (d, 1H, H-5', $J=8.3$), 7.01-7.22 (m, 5H, H-5, H-6, H-7, H-2', H-6'), 8.03 (s, 1H, H-4), 9.07 (s, 1H, OH), 9.22 (s, 1H, OH), 10.16 (s, 1H, OH). ^{13}C NMR ($DMSO-d_6$) δ (ppm): 115.5, 116.2, 117.6, 118.5, 120.0, 120.8, 124.6, 125.9, 126.8, 138.8, 139.0, 145.0, 146.3, 155.2, 164.8. MS m/z (%): 271 (18), 270 (M^+ , 100). Ana. Elem. Calc. for $C_{15}H_{10}O_5$: C, 66.67; H, 3.73. Found: C, 66.66; H, 3.71.

Compounds 1, 2, 5, 6, 10, 11, 15, 16, 17, 23, 24 and 27 have been previously described.^{23,24,25,41,42,43,44,45,46}

Adenosine receptors affinity. The affinity of the studied compounds for the human adenosine receptor subtypes hA_1 , hA_{2A} and hA_3 , was determined with radioligand competition experiments in Chinese hamster ovary (CHO) cells that were stably transfected with the individual receptor subtypes. The radioligands used were 1 nM [3H]CCPA for hA_1 , 10 nM [3H]NECA for hA_{2A} , and 1 nM [3H]HEMADO for hA_3 receptors. The results were expressed as K_i values (dissociation constants), which were calculated with the program Prism (GraphPad Software). K_i values are reported as geometric means of three independent experiments with each tested concentration of compound measured in duplicate. As an interval estimate for the dissociation constants, 95% confidence intervals are given in parentheses. Details for pharmacological experiments are described in previous works.^{26,29} Due to the lack of a suitable radioligand for hA_{2B} receptors, the potency of antagonists at the hA_{2B} receptor (expressed on CHO cells) was determined by inhibition of NECA-stimulated adenylyl cyclase activity.

GloSensor cAMP Assay. Functional A_3 adenosine receptor activity was determined using a biosensor technology called GloSensor cAMP assay. It consists of a mutant form of Firefly luciferase into which a cAMP-binding protein moiety has been inserted. When the cAMP binds the biosensor there is a conformational change which induce an increase of light output that allow to evaluate the activity of ligands at the receptor under study. Briefly, cells stably expressing the hA_3 adenosine receptor and transiently the biosensor, were harvested and incubated in equilibration medium containing a 3% v/v GloSensor cAMP reagent stock solution, 10% FBS, and 87% CO_2 independent medium. After 2 h of incubation at room temperature, cells were dispensed in the wells of a 384-well plate and NECA reference agonist or the understudy compounds, at different concentrations,

1
2
3 were added. When compounds were unable to inhibit the cAMP production they were
4
5 studied as antagonists. In particular, the antagonist profile was evaluated by assessing the
6
7 ability of these compounds to counteract NECA-induced decrease of cAMP
8
9 accumulation. Responses were expressed as percentage of the maximal relative
10
11 luminescence units (RLU). Concentration–response curves were fitted by a nonlinear
12
13 regression with the Prism 5.0 programme (GraphPAD Software, San Diego, CA, USA).
14
15 The antagonist profile of the compounds was expressed as IC_{50} , which is the
16
17 concentration of antagonists that produces 50% inhibition of the agonist effect. Three
18
19 independent experiments with each tested concentration of compound measured five
20
21 times. The final values are given with 95% confidence intervals.³¹
22
23
24
25
26
27

28 **hA₃ homology model.** Homology model of hA₃ receptor along with a description of its
29
30 construction was previously published by our group.^{21,32} The hA_{2A} crystallized structure
31
32 (PDB code: 3EML)³⁴ was used as a template for the development of the homology model.
33
34 The alignment between both proteins was reported previously and it is included in
35
36 Katritch *et al.*,⁴⁷ considering highly conserved residues in the TMs. The Homology Model
37
38 module in MOE software was used to develop the hA₃ model.⁴⁸ For residues that are
39
40 identical, the heavy atoms coordinates are copied to the new target from the template,
41
42 whereas only the backbone is taken into account for different residues. The residues
43
44 placed in the loops with no specified coordinates are constructed based on high resolution
45
46 fragments available in the PDB. A Boltzmann-weighted function is used for the selection
47
48 of the loops. The top hA₃ model according to the Generalized Born/Volume Integral
49
50 (GB/VI) scoring was selected. The geometrical quality of Phi-Psi dihedrals, bond
51
52 lengths, bond angles, dihedrals, side chains and non-bonded interactions was assessed
53
54 with the Protein Geometry module. Protein pocket was optimized by docking high
55
56
57
58
59
60

affinity ligands using the Induced Fit Docking workflow allowing flexibility in the pocket residues.³³ The best hA₃ homology models showed ROC curves greater than 0.80 in the discrimination of ligands from decoys. A detailed description of the homology modeling was provided in previous studies.^{21,32}

Moreover, our hA₃ receptor was compared to a model generated using the protein structure homology model server SwissModel.⁴⁹ The server automatically detected the hA₁ (PDB code: 5UEN)⁵⁰ as the best template and generated a hA₃ model that is in agreement with our reported homology model using as a template the hA_{2A} receptor (PDB code: 3EML). The average RMSD between both models is 2.8 Å whereas the RMSD between both pockets is 0.9 Å. More details about homology model comparison are provided in the Supporting Information.

Molecular docking. Molecular docking simulations in the hA₃ and hA_{2A} proteins were run using the Schrödinger package.³³ Ligands were prepared with the LigPrep module that included the next steps: generation of tautomers and different protonation states (pH=7±2) and optimization of the molecular structures. Protein structures were also prepared with the module Protein Preparation Wizard to optimize protonation states of some residues and the H-bond network of the proteins. After this step, a grid centered in the pocket was generated (*van der Waals* radius scaling=1.0; partial charge cut-off=0.25). The ligands were docked to the hA₃ and hA_{2A} using Glide standard precision (SP mode). Top scoring function poses were selected as representative of the simulations.

AUTHOR INFORMATION

Corresponding Authors

* Maria J. Matos: phone, +34 881814936; E-mail, mariajoao.correiapinto@usc.es or maria.matos@fc.up.pt.

* Fernanda Borges: phone, +351 220402560; E-mail, fborges@fc.up.pt.

ORCID

Maria J. Matos: 0000-0002-3470-8299

S. Vilar: 0000-0003-2663-4370

S. Vazquez-Rodriguez: 0000-0003-1356-8984

K.-N. Klotz: 0000-0003-3553-3205

M. Buccioni: 0000-0002-8383-0813

G. Delogu: 0000-0003-0307-1544

L. Santana: 0000-0001-6056-8253

E. Uriarte: 0000-0001-6218-2899

F. Borges: 0000-0003-1050-2402

Author Contributions

M.J.M., E.U. and F.B. conceived and supervised the study. M.J.M., S.V.-R. and G.D. performed the synthesis, purification and characterization of the compounds. E.U. and L.S. co-supervised the synthetic part of the work. S.K. and M.B. performed the pharmacological assays on adenosine receptors. K.-N.K. supervised and validated the pharmacological assays. S.V. performed the docking studies. L.S. and F.B. co-supervised the modelling studies. M.J.M. wrote the manuscript with contributions from all authors. All authors approved the final version of the manuscript.

Notes

The authors declare no competing financial interest.

ACKNOWLEDGEMENTS

This work was partially supported by University of Porto and University of Santiago de Compostela. Authors would like to thank the use of RIAIDT-USC analytical facilities. This project has received funding from the European Union's Horizon 2020 research and innovation programme under the Marie Skłodowska-Curie grant agreement No 744389, supporting S.V.R. postdoctoral fellowship (TEDCIP). Authors would like to thank Angeles Alvariño Plan Galego de Investigación, Innovación e Crecemento 2011–2015 (S.V.), European Social Fund, FCT, POPH, and QREN (SFRH/BPD/95345/2013, M.J.M.) for funding. This project has received funding from Xunta da Galicia and Galician Plan of Research, Innovation and Growth 2011–2015 (Plan I2C, ED481B 2014/086–0 and ED481B 2018/007, M.J.M.). This project was supported by Foundation for Science and Technology (FCT), and FEDER/COMPETE (POCI-01-0145-FEDER-006980). This article is based upon work from COST Action CA15135.

ABBREVIATIONS USED

K_i , dissociation constant; GPCR, G protein-coupled receptors; DCC, *N,N'*-dicyclohexylcarbodiimide; Ac_2O , acetic anhydride; MeOH, methanol; AcOH, acetic acid; μM , micromolar; PDB, protein data bank; SP, Glide standard precision; RMSD, root mean square deviation; FC, flash chromatography; CHO cells, Chinese hamster ovary cells. [^3H]CCPA, (2R,3R,4S,5R)-2-(2-Chloro-6-cyclopentylamino-purin-9-yl)-5-hydroxymethyl-tetrahydro-3,4-diol); [^3H]NECA, (1-(6-amino-9*H*-purin-9-yl)-1-deoxy-*N*-ethyl- β -dribofuronamide); [^3H]HEMADO, 2-(1-hexynyl)-*N*⁶-methyladenosine [^3H]; MOE, molecular operating environment; GB, generalized born; VI, volume integral; ROC, receiver operating characteristic.

ASSOCIATED CONTENT

* Supporting Information

The Supporting Information is available free of charge on the ACS Publications website at DOI: XXX. Supporting Information includes Rationale for this study, Crystallographic data of compound **4**, Docking information for compound **4**, Representative hA₃ homology models and HPLC trace for compound **4**. Molecular Formula Strings are also available.

REFERENCES

- ¹ Sheth, S.; Brito, R.; Mukherjea, D.; Rybak, L. P.; Ramkumar, V. Adenosine Receptors: Expression, Function and Regulation. *Inter. J. Molec. Sci.* **2014**, *15*(2), 2024–2052.
- ² Fredholm, B. B.; IJzerman, A. P.; Jacobson, K. A.; Linden, J.; Müller, C. E. International Union of Basic and Clinical Pharmacology. LXXXI. Nomenclature and Classification of Adenosine Receptors—an Update. *Pharmacol. Rev.* **2011**, *63*(1), 1.
- ³ Gao, Z.-G.; Verzijl, D.; Zweemer, A.; Ye, K.; Göblyös, A.; IJzerman, A. P.; Jacobson, K. A. Functionally Biased Modulation of A₃ Adenosine Receptor Agonist Efficacy and Potency by Imidazoquinolinamine Allosteric Enhancers. *Bioch. Pharmacol.* **2011**, *82*(6), 658–668.
- ⁴ Chen, J. F.; Eltzschig, H. K.; Fredholm, B.B. Adenosine Receptors as Drug Targets – What are the Challenges? *Nat. Rev. Drug Discov.* **2013**, *12*(4), 265–86.
- ⁵ St Hilaire, C.; Carroll, S. H.; Chen, H.; Ravid, K. C. Mechanisms of Induction of Adenosine Receptor Genes and its Functional Significance. *J. Cell Physiol.* **2009**, *218*(1), 35–44.
- ⁶ Baraldi, P.; Tabrizi, M.; Gessi, S.; Borea, P. Adenosine Receptor Antagonists: Translating Medicinal Chemistry and Pharmacology into Clinical Utility. *Chem. Rev.* **2008**, *108*, 238–263.

-
- ⁷ Jacobson, K. A.; Müller, C. E. Medicinal Chemistry of Adenosine, P2Y and P2X Receptors. *Neuropharmacology* **2016**, *104*, 31–49.
- ⁸ Mizuno, Y.; Hasegawa, K.; Kondo, T.; Kuno, S.; Yamamoto, M. Clinical Efficacy of Istradefylline (KW-6002) in Parkinson's Disease: A Randomized, Controlled Study. *Mov. Disord.* **2010**, *25*(10), 1437–1443.
- ⁹ Sousa, J. B.; Diniz, C. The Adenosinergic System as a Therapeutic Target in The Vasculature: New Ligands and Challenges. *Molecules* **2017**, *22*(5), 752–779.
- ¹⁰ Vecchio, E. A.; Baltos, J. A.; Nguyen, A. T. N.; Christopoulos, A.; White, P. J.; May, L.T. New Paradigms in Adenosine Receptor Pharmacology: Allostery, Oligomerization and Biased Agonism. *Br. J. Pharmacol.* **2018**, *175*(21), 4036–4046.
- ¹¹ Melani, A.; Pugliese, A. M.; Pedata, F. Adenosine Receptors in Cerebral Ischemia. *Int. Rev. Neurobiol.* **2014**, *119*, 309–348.
- ¹² Rivkees, S. A.; Thevananther, S.; Hao, H. Are A3 Adenosine Receptors Expressed in the Brain? *Neuroreport.* **2000**, *11*(5), 1025–1030.
- ¹³ Borea, A. P.; Varani, K.; Vincenzi, F.; Baraldi, P. G.; Tabrizi, M. A.; Merighi, S.; Gessi, S. The A3 Receptor: History and Perspectives. *Pharmacol. Rev.* **2015**, *67*(1), 74–102.
- ¹⁴ Fishman, P.; Cohen, S. The A3 Adenosine Receptor (A3AR): Therapeutic Target and Predictive Biological Marker in Rheumatoid Arthritis. *Clin. Rheumatol.* **2016**, *35*(9), 2359–2362.
- ¹⁵ Bagatini, M. D.; Dos Santos, A. A.; Cardoso, A. M.; Mânica, A.; Reschke, C. R.; Carvalho, F. B. The Impact of Purinergic System Enzymes on Noncommunicable, Neurological, and Degenerative Diseases. *J. Immunol. Res.* **2018**, 4892473.
- ¹⁶ Vazquez-Rodriguez, S.; Matos, M. J.; Santana, L.; Uriarte, E.; Borges, F.; Kachler, S.; Klotz, K.-N. Chalcone-Based Derivatives as New Scaffolds for Ha3 Adenosine Receptor Antagonists. *J. Pharm. Pharmacol.* **2013**, *65*, 697–703.

- ¹⁷ Fonseca, A.; Matos, M. J.; Vilar, S.; Kachler, S.; Klotz, K.-N.; Uriarte, E.; Borges, F. Coumarins and Adenosine Receptors: New Perceptions in Structure-Affinity Relationships. *Chem. Biol. Drug Des.* **2018**, *91*, 245–256.
- ¹⁸ Matos, M. J.; Hogger, V.; Gaspar, A.; Kachler, S.; Borges, F.; Uriarte, E.; Santana, L.; Klotz, K.-N. Synthesis and Adenosine Receptors Binding Affinities of a Series of 3-Arylcoumarins. *J. Pharm. Pharmacol.* **2013**, *65*, 1590–1597.
- ¹⁹ Matos, M. J.; Gaspar, A.; Kachler, S.; Klotz, K.-N.; Borges, F.; Santana, L.; Uriarte, E. Targeting Adenosine Receptors with Coumarins: Synthesis and Binding Activities of Amide and Carbamate Derivatives. *J. Pharm. Pharmacol.* **2013**, *65*, 30–34.
- ²⁰ Matos, M. J.; Vilar, S.; Kachler, S.; Celeiro, M.; Vazquez-Rodriguez, S.; Santana, L.; Uriarte, E.; Hripcsak, G.; Borges, F.; Klotz, K.-N. Development of Novel Adenosine Receptor Ligands Based on the 3-Amidocoumarin Scaffold. *Bioorg. Chem.* **2015**, *61*, 1–6.
- ²¹ Matos, M. J.; Vilar, S.; Kachler, S.; Fonseca, A.; Santana, L.; Uriarte, E.; Borges, F.; Tatonetti, N. P.; Klotz, K.-N. Insight into the Interactions Between Novel Coumarin Derivatives and Human A3 Adenosine Receptors. *ChemMedChem* **2014**, *9*, 2245–2253.
- ²² Matos, M. J.; Varela, C.; Vilar, S.; Hripcsak, G.; Borges, F.; Santana, L.; Uriarte, E.; Fais, A.; Di Petrillo, A.; Pintus, F.; Era, B. Design and Discovery of Tyrosinase Inhibitors Based on a Coumarin Scaffold. *RSC Adv.* **2015**, *5*, 94227–94235.
- ²³ Matos, M. J.; Santana, L.; Uriarte, E.; Delogu, G.; Corda, M.; Fadda, M. B.; Era, B.; Fais, A. New Halogenated Phenylcoumarins as Tyrosinase Inhibitors. *Bioorg. Med. Chem. Lett.* **2011**, *21(11)*, 3342–3345.
- ²⁴ Viña, D.; Matos, M. J.; Ferino, G.; Cadoni, E.; Laguna, R.; Borges, F.; Uriarte, E.; Santana, L. 8-Substituted 3-Arylcoumarins as Potent and Selective MAO-B Inhibitors:

- Synthesis, Pharmacological Evaluation, and Docking Studies. *ChemMedChem* **2012**, *7*(3), 464–470.
- ²⁵ Matos, M. J.; Perez-Cruz, F.; Vazquez-Rodriguez, S.; Uriarte, E.; Santana, L.; Borges, F.; Olea-Azar, C. Remarkable Antioxidant Properties of a Series of Hydroxy-3-Arylcoumarins. *Bioorg. Med. Chem.* **2013**, *21*(13), 3900–3906.
- ²⁶ Matos, M. J. CCDC 1937910: Experimental Crystal Structure Determination. *CSD Commun.* **2019**, DOI: 10.5517/ccdc.csd.cc231k7z.
- ²⁷ Matos, M. J.; Santana, L.; Uriarte, E. 3-Phenylcoumarin. *Acta Cryst.* **2012**, *E68*, o2645.
- ²⁸ Klotz, K.-N.; Hessling, J.; Hegler, J.; Owman, C.; Kull, B.; Fredholm, B. B.; Lohse, M. J. Comparative Pharmacology of Human Adenosine Receptor Subtypes - Characterization of Stably Transfected Receptors in CHO Cells. *Naunyn Schmiedeberg's Arch. Pharmacol.* **1997**, *357*, 1–9.
- ²⁹ Klotz, K.-N.; Falgner, N.; Kachler, S.; Lambertucci, C.; Vittori, S.; Volpini, R.; Cristalli, G. [3H]HEMADO—a novel Tritiated Agonist Selective for the Human Adenosine A3 Receptor. *Eur. J. Pharmacol.* **2007**, *556*, 14–18.
- ³⁰ Gazoni, L. M.; Walters, D. M.; Unger, E. B.; Linden, J.; Kron, I. L.; Laubach, V. E. Activation of A1, A2A, or A3 Adenosine Receptors Attenuates Lung Ischemia-Reperfusion Injury. *J. Thorac. Cardiovasc. Surg.* **2010**, *140*(2), 440–446.
- ³¹ Buccioni, M.; Marucci, G.; Dal Ben, D.; Giacobbe, D.; Lambertucci, C.; Soverchia, L.; Thomas, A.; Volpini, R.; Cristalli, G. Innovative Functional cAMP Assay for Studying G Protein-Coupled Receptors: Application to the Pharmacological Characterization of GPR17. *Purinerg. Signal.* **2011**, *7*, 463–468.
- ³² Cagide, F.; Gaspar, A.; Reis, J.; Chavarria, D.; Vilar, S.; Hripcsak, G.; Uriarte, E.; Kachler, S.; Klotz, K.-N.; Borges, F.; Navigating in Chromone Chemical Space:

Discovery of Novel and Distinct A3 Adenosine Receptor Ligands. *RSC Adv.* **2015**, 5, 78572–78585.

³³ Schrödinger suite 2014-3, Schrödinger, LLC, New York, USA, 2014. Available at: <http://www.schrodinger.com/>.

³⁴ Jaakola, V. P.; Griffith, M. T.; Hanson, M. A.; Cherezov, V.; Chien, E. Y.; Lane, J. R.; Ijzerman, A. P.; Stevens, R. C. The 2.6 Angstrom Crystal Structure of a Human A2A Adenosine Receptor Bound to an Antagonist. *Science* **2008**, 322, 1211–1217.

³⁵ Congreve, M.; Andrews, S. P.; Doré, A. S.; Hollenstein, K.; Hurrell, E.; Langmead, C. J.; Mason, J. S.; Ng, I. W.; Tehan, B.; Zhukov, A.; Weir, M.; Marshall, F. H. Discovery of 1,2,4-Triazine Derivatives as Adenosine A2A Antagonists Using Structure Based Drug Design. *J. Med. Chem.* **2012**, 55, 1898–1903.

³⁶ Jaakola, V. P.; Lane, J. R.; Lin, J. Y.; Katritch, V.; Ijzerman, A. P.; Stevens, R. C. Ligand Binding and Subtype Selectivity of the Human A2A Adenosine Receptor: Identification and Characterization of Essential Amino Acid Residues. *J. Biol. Chem.* **2010**, 285, 13032–13044.

³⁷ Gaspar, A.; Reis, J.; Kachler, S.; Paoletta, S.; Uriarte, E.; Klotz, K.-N.; Moro, S.; Borges, F. Discovery of Novel A3 Adenosine Receptor Ligands Based on Chromone Scaffold. *Biochem. Pharmacol.* **2012**, 84(1), 21–29.

³⁸ Alcaro, S.; Coleman, R. S. A Molecular Model for DNA Cross-Linking by the Antitumor Agent Azinomycin B. *J. Med. Chem.* **2000**, 43(15), 2783–2788.

³⁹ Perola, E.; Charifson, P. S. Conformational Analysis of Drug-Like Molecules Bound to Proteins: An Extensive Study of Ligand Reorganization upon Binding. *J. Med. Chem.* **2004**, 47(10), 2499–2510.

- ⁴⁰ Schiebel, J.; Gaspari, R.; Wulsdorf, T.; Ngo, K.; Sohn, C.; Schrader, T. E.; Cavalli, A.; Ostermann, A.; Heine, A.; Klebe, G. Intriguing Role of Water in Protein-Ligand Binding Studied by Neutron Crystallography on Trypsin Complexes. *Nat. Commun.* **2018**, *9*(1), 3559.
- ⁴¹ Walki, S.; Naveen, S.; Kenchanna, S.; Mahadevan, K. M.; Kumara, M. N.; Lokanath, N. K. Crystal Structure of 8-Ethoxy-3-(4-nitrophenyl)-2*H*-chromen-2-one. *Acta Crystallogr. E Crystallogr. Commun.* **2015**, *71*(11), o860–o861.
- ⁴² Valenti, P.; Rampa, A.; Budriesi, R.; Bisi, A.; Chiarini, A. Coumarin 1,4-Dihydropyridine Derivatives. *Bioorg. Med. Chem.* **1998**, *6*, 803–810.
- ⁴³ Nemeryuk, M. P.; Dimitrova, V. D.; Sedov, A. L.; Anisimova, O. S.; Traven, V. F. New Approach to the Synthesis of 3-Arylcoumarins. Reaction of 3-Acyl and 3-Ethoxycarbonyl-Coumarins with Hydrazide of *p*-Nitrophenylacetic Acid. *Chem. Heteroc. Comp.* **2002**, *38*(2), 249–250.
- ⁴⁴ Jafarpour, F.; Zarei, S.; Olia, M. B. A.; Jalalimanesh, N.; Rahiminejadan, S. Palladium-Catalyzed Decarboxylative Cross-Coupling Reactions: A Route for Regioselective Functionalization of Coumarins. *J. Org. Chem.* **2013**, *78*, 2957–2964.
- ⁴⁵ Bulut, M.; Erk, C. The Synthesis of Novel Crown Ethers, Part IX, 3-Phenyl Chromenone-Crown Ethers. *J. Heteroc. Chem.* **2001**, *38*(6), 1291–1295.
- ⁴⁶ Gunduz, C.; Bulut, M. Synthesis of 7,8-Dihydroxy-3-(3,4-dihydroxyphenyl)-2*H*-chromen-2-one Derivatives of Crown Ethers. *J. Heteroc. Chem.* **2009**, *46*(1), 105–107.
- ⁴⁷ Katritch, V.; Kufareva, I.; Abagyan, R. Structure Based Prediction of Subtype-Selectivity for Adenosine Receptor Antagonists. *Neuropharmacology* **2011**, *60*, 108–115.
- ⁴⁸ MOE, version 2011.10; Chemical Computing Group, Inc.: Available at: <http://www.chemcomp.com>.

-
- ⁴⁹ Waterhouse, A.; Bertoni, M.; Bienert, S.; Studer, G.; Tauriello, G.; Gumienny, R.; Heer, F. T.; de Beer, T. A. P.; Rempfer, C.; Bordoli, L.; Lepore, R.; Schwede, T. SWISS-MODEL: Homology Modelling of Protein Structures and Complexes. *Nucleic Acids Res.* **2018**, *46(W1)*, W296–W303.
- ⁵⁰ Glukhova, A.; Thal, D. M.; Nguyen, A. T.; Vecchio, E. A.; Jörg, M.; Scammells, P. J.; May, L. T.; Sexton, P. M.; Christopoulos, A. Structure of the Adenosine A1 Receptor Reveals the Basis for Subtype Selectivity. *Cell* **2017**, *168(5)*, 867–877.

Table of Contents graphic

